



# Excited High-Spin Quartet ( $S = 3/2$ ) State of a Novel $\pi$ -Conjugated Organic Spin System, Pyrene–Verdazyl Radical

Yoshio Teki,\* Mituhiro Kimura, Shinsuke Narimatsu,<sup>1</sup> Keishi Ohara,<sup>1</sup> and Kazuo Mukai\*,<sup>1</sup>

Department of Material Science, Graduate School of Science, Osaka City University,  
3-3-138 Sugimoto, Sumiyoshi-ku, Osaka 558-8585

<sup>1</sup>Department of Chemistry, Faculty of Science, Ehime University, Bunkyo-cho 2-5, Matsuyama 790-8577

Received July 28, 2003; E-mail: teki@sci.osaka-cu.ac.jp

The excited high-spin quartet ( $S = 3/2$ ) state of the intramolecular triplet–radical pair between the excited triplet state of pyrene and a dangling verdazyl radical was reported. A novel verdazyl radical with the pyrene moiety was designed and synthesized. The time-resolved ESR spectrum and a DFT calculation show the photo-induced ferromagnetic spin alignment between the excited triplet state of the pyrene moiety and the dangling verdazyl radical. This is the first observation of the high-spin ( $S > 1$ ) excited state of the  $\pi$ -conjugated pyrene–radical pair.

The photo-induced spin alignment through  $\pi$ -conjugation is one of the key processes for photo-control of the molecule-based magnetism. We have recently reported the photo-excited quartet ( $S = 3/2$ ) and quintet ( $S = 2$ ) states on purely organic  $\pi$ -conjugated radical–triplet pair systems, which were generated by a spin alignment through  $\pi$ -conjugation between dangling imino-nitroxide radicals ( $S = 1/2$ ) and the excited triplet ( $S = 1$ ) state of a phenyl- or diphenylanthracene.<sup>1–5</sup>  $\pi$ -Conjugated spin systems arising from the aromatic hydrocarbons and the stable radicals are ideal systems on studying the photo-induced intramolecular spin alignment through  $\pi$ -conjugation. The spin correlation of their unpaired electrons via the delocalized  $\pi$  orbital network is the most important for determining the spin states both in the ground states<sup>6</sup> and in the photo-excited states.<sup>2</sup>

Some kinds of the excited high-spin systems arising from the radical–triplet pairs were reported since the pioneering works of Corvaja et al.<sup>7</sup> and Yamauchi et al.<sup>8</sup> However, the number of the literatures is still limited<sup>1–5,7–15</sup> and, in the almost all studies of their excited high-spin states, stable nitroxide radicals were used as a spin origin. For purely organic excited high-spin systems, only fullerene-nitroxide<sup>7,9,11,12</sup> and anthracene derivatives<sup>1–5</sup> have been reported. The search for the novel photo-excited high-spin organic systems constructed from other radicals and other triplet moieties is an important research target. Only our previous works using the anthracene derivatives<sup>1–5</sup> offer unique examples of the high-spin excited states on the  $\pi$ -conjugated radical–triplet pair systems. Although a CIDEP (RTPM) arising from the exchange interaction between the excited triplet state of pyrene and a doublet spin of radical species was reported in solution,<sup>16</sup> there has been no direct observation of the excited high-spin state.

In this paper, we report on the photo-excited high-spin quartet ( $S = 3/2$ ) state of the novel  $\pi$ -conjugated spin system (**1**), which originates from the triplet state of pyrene and the dangling verdazyl radical. This is the first direct observation of the excited high-spin state of the pyrene-based triplet–radical

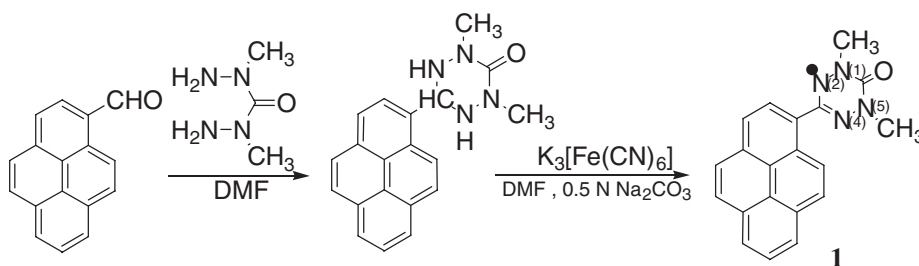
pair, in which a verdazyl radical couples to the triplet state of the pyrene moiety through  $\pi$ -conjugation. A novel verdazyl radical (**1**) was designed and synthesized. The photo-excited state has been investigated by time-resolved ESR. The spin-density distributions provide the most direct information about the spin correlation among the unpaired electrons and the mechanism of the spin alignment. The mechanism of the intramolecular spin alignment on the excited states has been discussed based on the spin-density distribution calculated by ab initio molecular orbital calculations.

## Experimental

**1. Materials.** As shown in Scheme 1, **1** was synthesized according to a procedure similar to that used by Neugebauer et al.<sup>17</sup> to prepare 1,5-dimethyl-3-phenyl-6-oxoverdazyl. The details of the synthetic procedures are omitted in this paper. Purification by silica-gel column chromatography using dichloromethane as a solvent gave **1** as dark-red powders: mp 223.5–224.5 °C (decomp.); Anal. Calcd for C<sub>20</sub>H<sub>15</sub>N<sub>4</sub>O: C, 73.38; H, 4.62; N, 17.11%. Found: C, 72.43; H, 4.93; N, 16.75%.

**2. Measurements and Analysis.** Absorption spectra were taken with a UV–vis spectrometer (Hitachi U-3000) at room temperature. Conventional ESR was measured by an X-band ESR spectrometer (JEOL-TE300) with a temperature control system (Oxford ESR 910). The ESR spectrum with hyperfine-splitting in solution was analyzed by a simulation according to the ordinary method. TRESR spectra were measured at 30 K using the JEOL-TE300 X-band ESR spectrometer. The details of the experimental setup are described in our previous paper.<sup>2</sup> Excitation was carried out at 500 nm light by an OPO laser system (Continuum Surelite OPO) pumped by a Nd:YAG laser (Continuum Surelite II-10). The typical laser power in this experiment was ca. 3–5 mJ. An EPA glass matrix was used for the TRESR experiments. Samples were degassed by repeated freeze-pump-thaw cycles using a high-vacuum line system.

The following ordinary spin Hamiltonian of a pure spin state was used for the analysis:



Scheme 1.

$$H'_{\text{spin}} = \beta_e \mathbf{H} \cdot \mathbf{g} \cdot \mathbf{S} + \mathbf{S} \cdot \mathbf{D} \cdot \mathbf{S} = \beta_e \mathbf{H} \cdot \mathbf{g} \cdot \mathbf{S} + D[S_Z^2 - S(S+1)/3] + E(S_X^2 - S_Y^2). \quad (1)$$

In order to determine the spin Hamiltonian parameters, full spectral simulation using Eq. 1 was carried out by the eigenfield/exact-diagonalization hybrid method,<sup>18,19</sup> taking the electron spin polarization (ESP) into account.

### Results and Discussion

**1. Conventional UV-vis and cw-ESR Spectra.** The UV-vis spectrum of **1** is shown in Fig. 1, together with a typical cw-ESR spectrum observed in a toluene solution at room temperature and in an EPA rigid glass matrix at 30 K. The absorption peaks in the wavelength region shorter than 370 nm come from the pyrene moiety. The very broad shoulder in the range of 370–550 nm is dominantly assigned to an  $n\pi^*$  transition of the dangling verdazyl radicals. Therefore, we can selectively

excite only the radical moiety by 500 nm light used in time-resolved ESR (TRESR) experiments. As shown in Fig. 1(b), a well-resolved hyperfine splitting of the four nitrogen atoms in the verdazyl moiety are observed in the solution ESR spectrum. The  $g$  value and the hyperfine splitting constants determined by the simulation are listed in Table 1. The spin-density distribution on the nitrogen atoms in the doublet ground state was also determined using the McConnell equation. The observed hyperfine splitting constants agree well with the calculated values using the ab initio MO calculation described in a latter section.

**2. TRESR Spectra and Excited Quartet State.** A typical TRESR spectrum observed at 0.5  $\mu$ s after laser excitation using the 500 nm light is shown in Fig. 2 together with a spectral simulation. This excitation wavelength corresponds to the  $n\pi^*$  transition of the radical moiety. A well-resolved fine-structure splitting was observed in this spectrum. The dominant nature of the TRESR spectrum was unambiguously analyzed to be

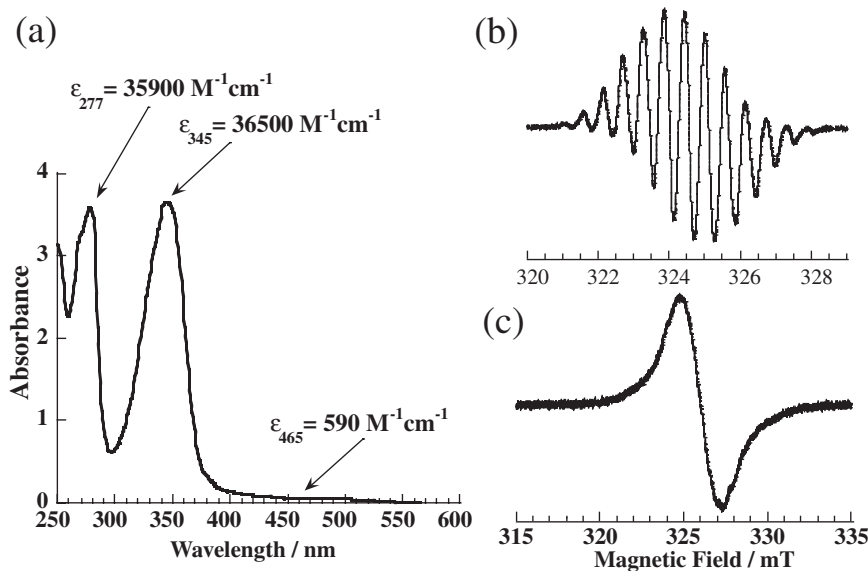


Fig. 1. Optical spectrum and X-band ESR spectra of **1**. (a) UV-vis spectrum observed at room temperature. (b) ESR spectrum in toluene solution. (c) ESR spectrum at 30 K in a rigid glass matrix. The microwave frequency is 9088.04 MHz.

Table 1.  $g$  Values and Hyperfine Splitting Constants of the Doublet Ground State of **1**

	$g$	hfcc/mT	$\pi$ Spin density
D	2.0038	$a_{N(2)} = a_{N(4)} = 1.20$ (calcd 1.07) <sup>a)</sup> $a_{N(1)} = a_{N(5)} = 0.62$ (calcd 0.58) <sup>a)</sup>	0.420 <sup>b)</sup> (calcd 0.438) 0.217 <sup>b)</sup> (calcd 0.191)

a) The values in the bracket are calculated ones by the ab initio MO calculation described in text.

b) The spin densities were estimated using the McConnell relation,  $A_N = Q_N \rho$  ( $Q_N = 2.86$  mT).<sup>20</sup>

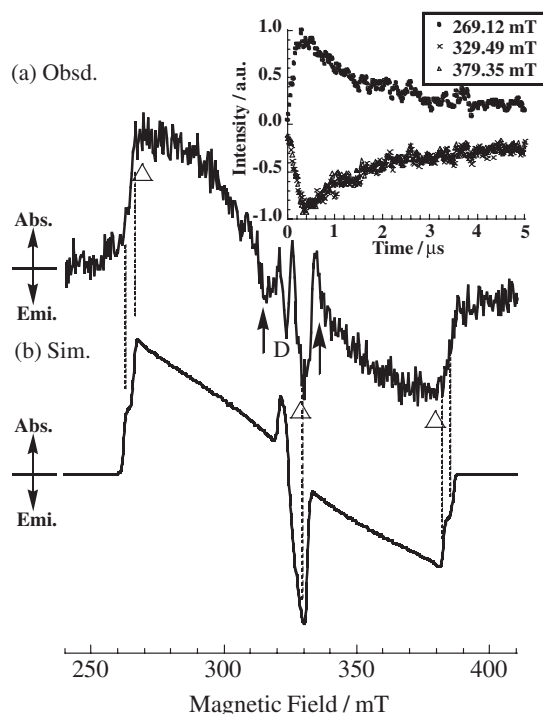


Fig. 2. Typical TRESR spectra of **1**. (a) Observed spectrum at 0.5  $\mu$ s after the laser excitation at 30 K in an EPA glass matrix. The microwave frequency is 9091.71 MHz. "D" denotes the signal due to the doublet ground state. The inset shows the time-profile of the signal intensities at the field positions shown in the inset. The field positions are also indicated in the observed spectrum by the symbol ( $\Delta$ ). (b) Simulated spectrum of the excited quartet state.

an excited quartet ( $S = 3/2$ ) high-spin state (Q) by the spectral simulation. The determined spin Hamiltonian parameters are listed in Table 2 together with the relative population of the  $M_S$  sublevels. We also carried out TRESR experiments by excitation of the  $\pi\pi^*$  transition of the pyrene moiety using 355 nm light of the Nd:YAG laser. In this case, the signals of the decomposed unknown impurity (indicated by arrows) was superposed in the quartet spectrum (not shown). The superposition of the impurity signals could be suppressed by the selective excitation of the  $n\pi^*$  transition using the OPO laser system, although a small amount of the spectral contamination of the unknown compound remains, as indicated by the arrows in Fig. 2(a). This small contamination may have come from excitation of the tail of the  $\pi\pi^*$  transition of the pyrene moiety, or from the energy-transfer pathway through an exciplex of the pyrene-radical system.

The determined  $g$  value (2.0035) is close to the expected value ( $g(Q) = (2g(T) + g(R))/3$ ,  $g(T) = 2.003$ , and  $g(R) = 2.0041$ ) for a quartet state constructed by a triplet-radical

pair.<sup>21</sup> In the weak-coupled limit, the fine-structure parameters,  $D$  and  $E$ , of the excited quartet state could also be estimated to be  $D(Q) = 0.0310 \text{ cm}^{-1}$  and  $E(Q) = 0.0103 \text{ cm}^{-1}$  from the following equation by the procedures described in the next section:

$$D(Q) = (1/3)\{D(T) + D(RT)\}. \quad (2)$$

Here,  $D(T)$  is the  $D$  tensor of the excited triplet pyrene moiety and  $D(RT)$  is the dipolar interaction between the dangling radical spin and the triplet moiety. In this estimation, the experimentally determined fine-structure parameters, ( $D(T) = 0.0810 \text{ cm}^{-1}$  and  $E(T) = 0.0182 \text{ cm}^{-1}$ ), of the excited triplet state of the pyrene molecule<sup>22</sup> were used, and  $D(RT)$  was calculated by the point-dipole approximation. The details of this estimation are described in the next section. The experimentally determined  $D$  and  $E$  values are close to the estimated ones, but a slightly smaller. A small reduction of the magnitude of the  $D$  value can be expected from a slight delocalization of the unpaired spins in whole of the molecules through  $\pi$ -conjugation. The experimentally determined  $|E/D|$  value (0.310), that being sensitive to the molecular structure, is also close to the estimated value (0.332), indicating the observed spectrum certainly comes from molecule **1**. The emissive signal, denoted by 'D' in Fig. 2(a), is assigned to be the signal arising from the doublet ground state judging from its  $g$  value. No signal arising from the excited doublet spin state was detected in the present  $\pi$ -conjugated spin system. This means that the energy splitting between the lowest excited quartet state and the excited doublet spin state is sufficiently large. The time profiles of the quartet signals at each canonical resonance field position are also shown in the inset of Fig. 2. The time profile shows that the signal intensity become a maximum at ca. 0.4  $\mu$ s after laser excitation. Each signal shows a similar time-decay behavior, showing that all of the signals come from a unique quartet spin state. The averaged intersystem crossing rate was determined to be ca.  $5.7 \times 10^6 \text{ s}^{-1}$  by fitting the raising-curves in the time profiles.

**3. Calculation of the Fine-Structure Tensor.** In an estimation of the fine-structure parameters, we used the fine-structure tensor of the triplet state of pyrene, itself,<sup>22</sup> as  $D(T)$  in Eq. 2.  $D(RT)$  was calculated by a point-dipole approximation using the calculated spin densities of each moiety. The spin densities of the triplet state of the pyrene moiety and of the doublet state of the verdazyl radical moiety (not shown) were obtained by an open-shell RHF calculation (ORHF Becke 3LYP/6-31G) based on density functional theory (DFT).<sup>23</sup> The calculated spin-density distributions used in this estimation are shown in Fig. 3. The molecular structure of **1** was assumed to be planar, because the optimized molecular structures of both moieties were nearly planar. The calculated  $D(T)$  and  $D(RT)$  tensors were obtained in units of  $\text{cm}^{-1}$  by

Table 2.  $g$  Values and Zero-Field Splitting Parameters and ISC Ratio of the Quartet (Q) Excited States of **1**

	$S$	$g$	$D/\text{cm}^{-1}$	$E/\text{cm}^{-1}$	ISC ratio
Q	3/2	2.0035	0.029	0.009	$P_{+3/2}:P_{+1/2}:P_{-1/2}:P_{-3/2} = 0.0:0.5:0.5:0.0$

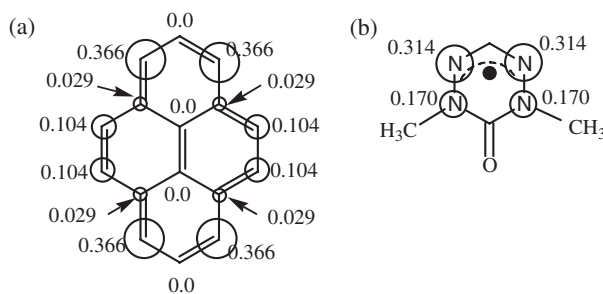


Fig. 3. Calculated spin density distributions. (a) Pyrene moiety. (b) Verdazyl radical unit.

$$D(T) = \begin{pmatrix} +0.0088 & 0.0 & 0.0 \\ 0.0 & -0.0540 & 0.0 \\ 0.0 & 0.0 & +0.0452 \end{pmatrix} \quad (3)$$

and

$$D(RT) = \begin{pmatrix} -0.0120 & +0.0133 & 0.0 \\ +0.0133 & -0.0047 & 0.0 \\ 0.0 & 0.0 & +0.0167 \end{pmatrix}. \quad (4)$$

The estimated  $D$  and  $E$  values were calculated by diagonalizing the fine-structure tensor given in Eq. 2 using these tensors. The obtained principal axis ( $Z$ ) giving the maximum fine-structure splitting was perpendicular to the molecular plane.

**4. Dynamic Electron Polarization Pathway.** The observed spectrum shows an absorptive and emissive ( $E$ ) pattern ( $A/E$  pattern) in the lower and higher magnetic field region than the  $g = 2$  position. This pattern is opposite to that of the spectral pattern of the triplet state of the pyrene molecule, itself (the TRESR spectrum of the triplet state of pyrene in the EPA glass was observed as a broad signal with an  $E/A$  pattern by 355 nm excitation). The relative population of the  $M_S$  sublevels in the excited quartet state is explained by the selective intersystem crossing (ISC) to the  $M_S = \pm 1/2$  spin sublevels in a zero magnetic field. The selective population in the quartet state observed in this experiment should be explained by the dynamic electron polarization pathway starting from the excited doublet state of the radical moiety. A plausible interpretation is illustrated in Fig. 4. An energy transfer occurs from the excited doublet state of the radical moiety ( $\psi_{D \pm 1/2}^{R*}$ ) to the  $n\pi^*$  excited

doublet state ( $\psi_{D \pm 1/2}^{n\pi*}$ ) generated by one-electron transfer from the lone-pair orbital ( $n$ ) of the nitrogen atom to the  $\pi^*$  orbital of the pyrene moiety. Then, the  $n\pi^*$  doublet state is relaxed to the  $\pi\pi^*$  excited quartet state ( $\psi_{Q \pm 1/2}^{\pi\pi*}$ ) by an enhanced intersystem crossing (ISC) mechanism induced by a  $\pi$ -conjugation between the  $\pi$  orbital of the pyrene moiety and the  $p\pi$  SOMO of the radical moiety. The origin of the ISC is spin-orbit coupling at the nitrogen atoms with the  $p\pi$  SOMO and the  $n$  orbital.<sup>2</sup> Here, although we omitted an explicit expression of the spin-orbit wavefunctions of these spin states, non-vanishing matrix elements of the energy transfer and the enhanced intersystem crossing pathways are  $\langle \pi | H_{e-e} | \text{SOMO}(N) \rangle$  and  $\xi \langle n | l_z | \text{SOMO}(N) \rangle \langle M_S' | s_z | M_S \rangle$ , respectively. Here,  $H_{e-e}$  is the electron-electron interaction,  $e^2/r_{ij}$ ,  $l_z$  and  $s_z$  are the  $z$  components of the local orbital angular momentum and the spin angular momentum operators in the one-center spin-orbit interaction ( $H_{so}$ ) at the nitrogen atom. Since both matrix elements do not change  $M_S$  value, the  $M_S$  conservation occurs during the whole spin-polarization transfer pathway, leading to the selective population of the  $M_S = \pm 1/2$  spin sublevels. A direct observation of the excited quartet state shows that a photo-induced intramolecular spin alignment is realized between the excited triplet state ( $S = 1$ ) of the pyrene moiety and the doublet spin ( $S = 1/2$ ) of the dangling verdazyl radical.

**5. Intramolecular Spin Alignment on the Excited Quartet State.** In order to clarify the physical picture of the intramolecular spin alignment, ab initio MO calculations for the excited quartet state and the doublet ground state were carried out based on DFT<sup>23</sup> using the full optimized energy minimum structures of each state obtained by the MNDO/AM1 method. In this calculation, the UHF method was suitable for clarifying the nature of the spin polarization. Therefore, the UBecke 3LYP hybrid method was used in the ab initio MO calculation. Figures 5(a) and 5(b) show the calculated spin densities of the doublet ground state and the excited quartet state, respectively. In the doublet ground state, the unpaired electron is almost localized in the verdazyl radical moiety. This is the result of strong twisting (almost perpendicular) between the molecular planes of the pyrene and the verdazyl radical moieties. On the other hand, the optimized molecular structure becomes more planar (the dihedral angle between the molecular planes is ca. 50 degrees) in the quartet photo-excited state. However, the magnitude of the spin density in the moiety is almost un-

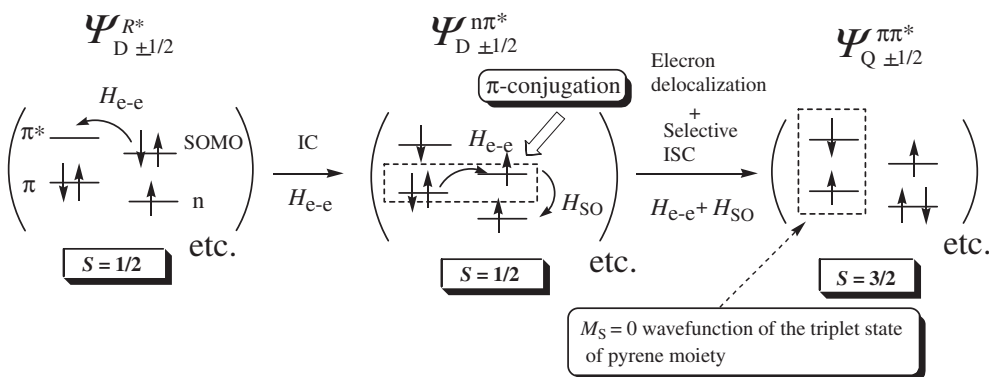


Fig. 4. Schematic illustration of the dynamic electron polarization pathway from the excited doublet state ( $\psi_{D \pm 1/2}^{R*}$ ) generated by the  $n\pi^*$  excitation of the radical moiety to the  $\pi\pi^*$  quartet state ( $\psi_{Q \pm 1/2}^{\pi\pi*}$ ).



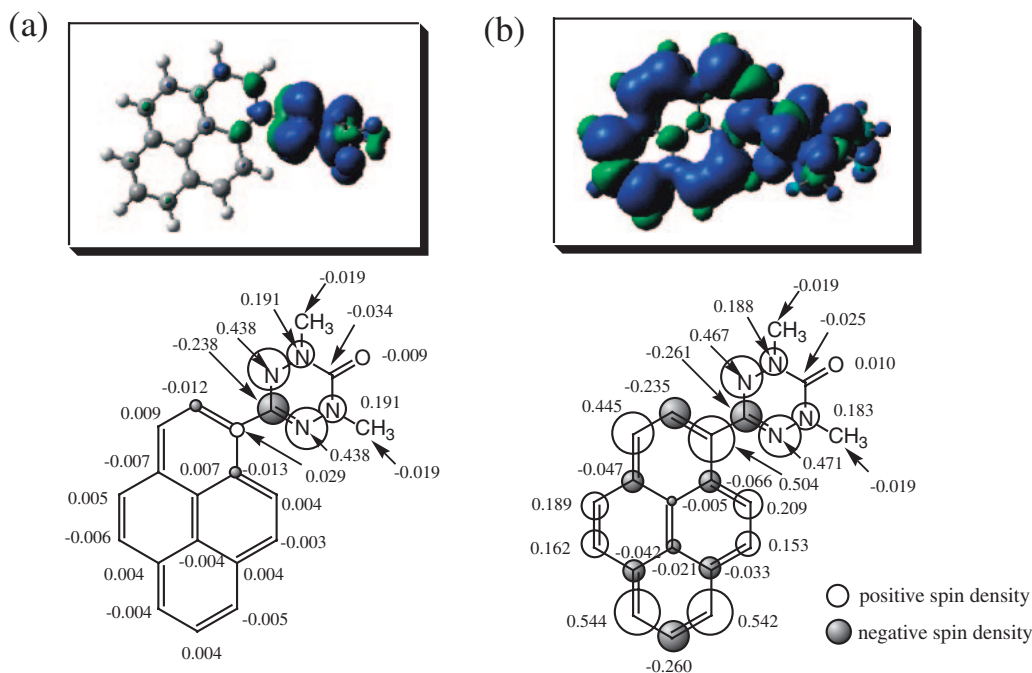


Fig. 5. Spin density distributions of **1** obtained by the ab initio MO calculation (UBecke 3LYP/STO 6-31G). (a) The doublet ground state. (b) The lowest excited quartet state.

changed in the excited quartet state. This result comes from Pauli's exclusion principle for unpaired electrons with the same spin direction. The calculation has clarified that the spin density of the pyrene moiety in the quartet state is dominantly generated by one-electron excitation from the  $\beta$ -HOMO ( $\pi$ ) to the  $\alpha$ -LUMO ( $\pi^*$ ) in the moiety. The connecting carbon site between their moieties has a large negative spin density ( $-0.261$ ). This shows that the large positive spin density ( $+0.504$ ) in the pyrene moiety couples to the large positive spin densities ( $+0.471$  and  $+0.467$ ) on the nitrogen atoms in the verdazyl moiety through the spin polarization mechanism. This large spin polarization effect through  $\pi$ -conjugation leads to a robust ferromagnetic spin coupling between the excited triplet spins and the dangling radical spin, giving the excited quartet high-spin state.

This work was the financial support by the Grant-in-Aid for Scientific Research (No. 13440211) from the Ministry of Education, Culture, Sports, Science and Technology.

## References

- Y. Teki, S. Miyamoto, K. Iimura, M. Nakatsuji, and Y. Miura, *J. Am. Chem. Soc.*, **122**, 984 (2000).
- Y. Teki, S. Miyamoto, M. Nakatsuji, and Y. Miura, *J. Am. Chem. Soc.*, **123**, 294 (2001).
- Y. Teki, M. Nakatsuji, and Y. Miura, *Int. J. Mod. Phys. B*, **15**, 4029 (2001).
- Y. Teki, *Polyhedron*, **20**, 1163 (2001).
- Y. Teki, M. Nakatsuji, and Y. Miura, *Mol. Phys.*, **100**, 1385 (2002).
- Ed by O. Kahn, *Mol. Cryst. Liq. Cryst.*, **334/335** (1999); "Proceedings of the VIth International Conference on Molecule-based Magnets," Seignosse, September 12–17 (1998).
- C. Corvaja, M. Maggini, M. Prato, G. Scorrano, and M. Venzin, *J. Am. Chem. Soc.*, **117**, 8857 (1995).
- K. Ishii, J. Fujiwara, Y. Ohba, and S. Yamauchi, *J. Am. Chem. Soc.*, **118**, 13079 (1996).
- C. Corvaja, M. Maggini, M. Ruzzi, G. Scorrano, and A. Toffoletti, *Appl. Magn. Reson.*, **12**, 477 (1997).
- K. Ishii, J. Fujisawa, A. Adachi, S. Yamauchi, and N. Kobayashi, *J. Am. Chem. Soc.*, **120**, 3152 (1998).
- P. Ceroni, F. Conti, C. Corvaja, M. Maggini, F. Paolucci, S. Roffia, G. Scorrano, and A. Toffoletti, *J. Phys. Chem. A*, **104**, 156 (2000), and references cited therein.
- N. Mizouchi, Y. Ohba, and S. Yamauchi, *J. Phys. Chem.*, **103**, 7749 (1999).
- K. Ishii, Y. Hirose, and N. Kobayashi, *J. Am. Chem. Soc.*, **120**, 10551 (1998).
- K. Ishii, Y. Hirose, and N. Kobayashi, *J. Phys. Chem.*, **103**, 1986 (1999).
- J. Fujiwara, Y. Iwasaki, Y. Ohba, S. Yamauchi, N. Koga, S. Karasawa, M. Fuhs, K. Möbbius, and S. Weber, *Appl. Magn. Reson.*, **21**, 483 (2001).
- A. Kawai and K. Obi, *J. Phys. Chem.*, **96**, 52 (1992).
- F. A. Neugebauer, H. Fisher, and R. Siegel, *Chem. Ber.*, **121**, 815 (1988).
- G. G. Belford, R. L. Belford, and J. F. Burkhalter, *J. Magn. Reson.*, **11**, 251 (1973).
- Y. Teki, I. Fujita, T. Takui, T. Kinoshita, and K. Itoh, *J. Am. Chem. Soc.*, **116**, 11499 (1994).
- P. H. H. Fischer, *Tetrahedron*, **23**, 1939 (1967).
- A. Bencini and D. Gatteschi, "EPR of Exchange Coupled Systems," Springer-Verlag, Berlin (1990).
- O. H. Griffith, *J. Phys. Chem.*, **69**, 1429 (1965). This paper was reported the triplet state of pyrene in a fluorine matrix.
- The DFT calculation was carried out using Gaussian 98, Revision A.11. Gaussian, Inc., Pittsburgh PA, 1998.